Energy Proceedings
Vol 51, 2025
ISSN 2004-2965

Experimental investigation of the effects of transverse vibration on the supercritical CO_2 heat transfer characteristics in a vertical/horizontal tube

Lin-Cheng Han[1], Jian Chen[2], Kun-Ru Wang[1], Hua Chen[1], Wen-Long Cheng[1*]

[1] Department of Thermal Science and Energy Engineering, University of Science and Technology of China, Hefei, Anhui, 230027, PR China

[2] China Ship Scientific Research Center, Wuxi, Jiangsu, 214082, PR China

([*]Corresponding Author: wlcheng@ustc.edu.cn (Wen-Long Cheng))

ABSTRACT

Heat transfer characteristics (*HTC*) of supercritical CO_2 (SCO_2) is crucial for many applications in the field of energy conversion. However, there are very few studies concerning the effects of vibration on the *HTC* of SCO_2. In this paper, the effects of transverse vibration on the *HTC* of SCO_2 flowing upward within a vertical tube (d=4.57 mm, L=1000 mm) are investigated experimentally and compared with a horizontal tube. The results reveal that vibration mitigates heat transfer deterioration (*HTD*) in the vertical tube, reduces the second peak of wall temperature along the channel significantly, and enhances heat transfer coefficient (*htc*). Vibration is more effective in enhancing heat transfer in the vertical tube compared to the horizontal tube. The vibration intensification mainly acts in the region before the mainstream enthalpy (h_b) reaches the pseudo-critical enthalpy (h_{pc}). Based on pseudo-boiling theory, vibration enhances heat transfer by inhibiting the growth of near-wall gas-like film and the temperature gradient inside the gas-like film.

Keywords: Supercritical CO_2, Vibration, Heat transfer characteristics, Heat transfer enhancement[1]

NONMENCLATURE

Abbreviations	
SCO_2	Supercritical CO_2
HTC	Heat transfer characteristics
HTE	Heat transfer enhancement
htc	Heat transfer coefficient
Symbols	
h	Enthalpy [kJ/kg]
P	Pressure [MPa]
G	Mass flux [kg/(m^2·s)]
q	Heat flux [kW/m^2]
T	Temperature[°C]
λ	Thermal conductivity [W/(m· K)]
ρ	Density [kg/m^3]
Subscripts	
b	Bulk
in	inlet
out	outlet
w	wall
pc	pseudo-critical

1. INTRODUCTION

CO_2, as an environmentally friendly natural medium, is extensively utilized in various energy conversion applications, such as waste heat recovery, solar/nuclear energy usage, geothermal systems, etc. [1]. The properties of CO_2 undergo drastic and nonlinear changes in the pseudo-critical region, leading to *HTD* and heat transfer enhancement (*HTE*) in the heat transfer process [2]. Energy conversion efficiency is essential for energy conservation, and the *HTC* of CO_2 is a key factor affecting the efficiency of energy conversion and utilization. Therefore, the research on the *HTC* of SCO_2 holds significant importance.

To analyze the SCO_2 *HTC* under different conditions, many scholars have carried out experimental studies on parameters affecting *HTC*. Li et al. [3] experimentally found that increasing the mass flow rate was beneficial in mitigating the *HTD*, resulting in a decrease in the peak wall temperature and a shift towards the high enthalpy region. Lei et al. [4] discovered that decreasing the mass flow rate at high heat flux improved heat transfer rather than worsened it. They concluded that the buoyancy effect intensifies heat transfer at low mass flow rates. Variations in heat flux can also lead to changes in heat transfer. Li et al. [3] revealed experimentally that the wall temperature showed a horizontal state along the channel when the heat flux was lower than 119.49 kW/m^2; the wall temperature existed in a localized peak when it exceeded 143.26 kW/m^2, there was a localized

This is a paper for the 16th International Conference on Applied Energy (ICAE2024), Sep. 1-5, 2024, Niigata, Japan.

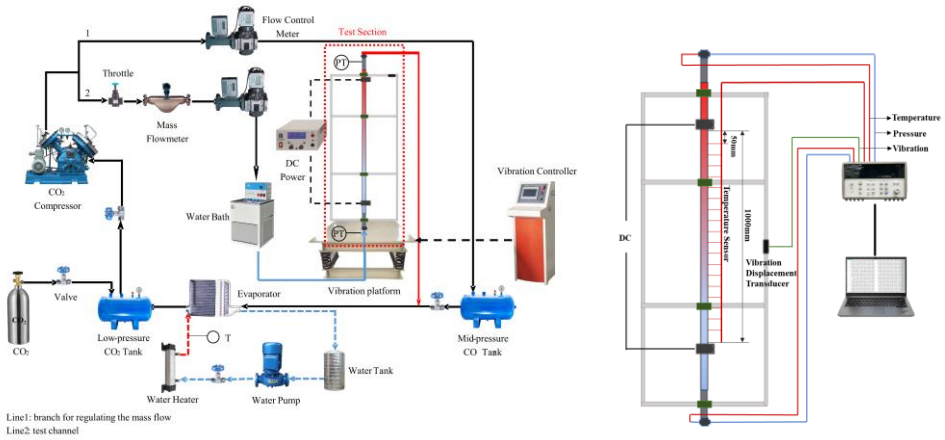

(a) (b)

Fig. 1 (a) Schematic diagram of the experimental facility; (b) Schematic diagram of the test section.

valley in the *htc*, and there is a *HTD*. Whereas, Jiang et al. [5] found that increasing the heat flux in a lower heat flux condition will instead increase the *htc*. Pressure has an effect on heat transfer by influencing the properties of SCO_2. Bae et al. [6] compared the heat transfer of SCO_2 at 7.75 MPa and 8.12 MPa and found lower wall temperatures and higher *htc* at the lower pressure. Experiments by Xu et al. [7] at 7.5 MPa, 8.5 MPa, and 9 MPa showed that the effects of pressure on *HTC* are more significant near the pseudo-critical point.

Many attempts have been made to alleviate *HTD*. The utilization of other shaped channels is a way to mitigate *HTD*, such as spiral runners, serpentine runners, etc. Zhang et al. [8] found that the peak of SCO_2 *htc* in spiral tubes increased by about 80% compared to vertical tubes and mitigated *HTD* in experiments. Chen et al. [9] experimentally found that rough walls contribute to mitigating *HTD* in vertical tubes. As the channel roughness grew, the peak wall temperature decreased, the deterioration range shortened, and the heat transfer performance improved significantly. Chen et al. [10] investigated the effects of adaptive runner structure on *HTC* by simulation. It was found that for the same heat transfer area, increasing the change length of the adaptive runner could mitigate *HTD*.

Inevitably, vibrations are faced when CO_2 is utilized as a work medium in automobiles, ships, and other types of mechanical equipment. However, few studies have been conducted on the *HTC* of CO_2 under vibration conditions. Our group preliminarily investigated the effects of transverse vibration on the *HTC* of CO_2 in a horizontal tube [11] . Since no *HTD* occurred under the experimental conditions, it was not feasible to demonstrate whether vibration could mitigate *HTD*. Therefore, it is necessary to investigate the effects of vibration on the *HTC* of CO_2 during upward flow in a vertical tube. In this paper, the *HTC* of CO_2 flowing upward in a vertical tube (d=4.57mm) under transverse vibration conditions was studied experimentally. The effects of static and vibration on the *HTC* were experimentally compared at different operating parameters when the test section was placed vertically and horizontally. The mechanism of vibration to mitigate *HTD* and enhance heat transfer in vertical tubes was further analyzed through the buoyancy effect and the pseudo-boiling theory.

2. EXPERIMENTS AND DATA REDUCTION

2.1 Experimental facility and test section

Fig. 1(a) shows the system flowchart of the SCO_2 *HTC* experiment. A vacuum pump is utilized to evacuate the system flow path to obtain a pressure of less than 10 Pa before the experiment. CO_2 with 99.99% purity is injected into a low-pressure CO_2 storage tank, and then the CO_2 is drawn from it and compressed into high-pressure CO_2 by a compressor. The high-pressure CO_2 is divided into two parts: a branch circuit (Line 1) that regulates the flow of the test circuit. The other is a test channel (Line 2) where CO_2 flows through a throttle valve and the pressure drops to the test range. A water bath is set up in front of the test section to regulate the CO_2 inlet temperature. Direct current (DC) is used to provide the required constant heat flux to the test section. Finally, the two parts converge and flow to the low-pressure tank, forming a cycle. The validation of the experimental system can be found in the previous work of our subject group [9, 11].

The schematic diagram of the test section is shown in Fig. 1(b). It is made of 316L stainless steel with a smooth inner wall surface. The inner and outer diameters of the tube are *d*=4.57 mm and *D*=6.35 mm, respectively, and the effective heating length *L*=1000 mm. A PT100 is installed at each of the inlet and outlet of the tube to

measure the CO_2 temperature. 21 groups of T-type thermocouples (along the vibration direction and perpendicular to the vibration direction as a cluster of temperature measurement points) are arranged at 50 mm intervals on the tube. The entire test section is wrapped in insulating cotton to minimize heat loss. The test section is fixed vertically on the vibration platform through an aluminum alloy frame, and the vibration amplitude and frequency are controlled by a controller. The inlet and outlet of the test section are connected by flexible pipes to avoid affecting the vibration effects of the test section due to fixed piping.

2.2 Data reduction

It is first necessary to determine the inner wall temperature and heat flux.

$$q = \frac{\eta IU}{\pi dL} \tag{1}$$

Where q is the heat flux through the inner wall; I and U are the current and voltage, respectively; and η is the heating efficiency (the ratio of heat absorbed by the fluid to the heat added), which is calculated as follows:

$$\eta = \frac{\dot{m}(h_{\text{out}} - h_{\text{in}})}{UI} \tag{2}$$

$\dot{m}$ is the mass flow rate; h_{in} and h_{out} are the enthalpy of CO_2 at the inlet and outlet, respectively; they can be obtained by the following formulas:

$$h_{\text{in}} = f(P, T_{\text{in}}), \quad h_{\text{out}} = f(P, T_{\text{out}}) \tag{3}$$

T_{in} and T_{out} are CO_2 inlet and outlet temperatures, respectively. The temperature of the wall inside the flow channel can be calculated by the equation:

$$T_{\text{w,i}}(x) = T_{\text{w,o}}(x) + \frac{q_{\text{v}}}{16\lambda_{\text{steel}}}(D^2 - d^2) + \frac{q_{\text{v}}}{8\lambda_{\text{steel}}} D^2 \ln\frac{d}{D} \tag{4}$$

Where $T_{\text{w,o}}$(x) is the outer wall temperature, obtained by averaging over a cluster of temperature measurement points; λ_{steel} is the thermal conductivity of stainless steel; q_{v} is the heat source per unit volume; they are calculated according to the following equations:

$$\lambda_{\text{steel}} = 14.408\left[1 + 0.0011332 T_{\text{w,o}}(x)\right] \tag{5}$$

$$q_{\text{v}} = \frac{IU}{\left[\pi\left(D^2 - d^2\right)L/4\right]} \tag{6}$$

Secondly, the mainstream temperature of the test section is calculated:

$$T_{\text{b}}(x) = f(P, h_{\text{b}}(x)) \tag{7}$$

Where P is the pressure and h_{b}(x) is the localized mainstream enthalpy of CO_2 along the flow channel, calculated as follows [4]:

$$h_{\text{b}}(x) = h_{\text{in}} + \frac{q\pi dx}{\dot{m}} = h_{\text{in}} + (h_{\text{out}} - h_{\text{in}}) \times \frac{x}{L} \tag{8}$$

x is the distance from the start of heating. Finally, the local heat transfer coefficient htc(x) along the channel can be found by the following equation:

$$htc(x) = \frac{q}{T_{\text{w,i}}(x) - T_{\text{b}}(x)} \tag{9}$$

2.3 Uncertainty analysis

PT100s are used to measure the inlet and outlet temperatures of the test section with an uncertainty of ±0.1 °C. The uncertainty of the type T thermocouple for measuring the outer wall temperature is ±0.2 °C. System pressure is measured by a Rosemount (3051) pressure sensor with an uncertainty of ±0.1%. The mass flow meter (Endress+Hauser 80A04) has an uncertainty of ±0.4%. The Keysight DC power supply (N8951, 0∼80 V, 0∼510 A) has voltage and current uncertainties of ±0.1% and ±0.2%, respectively. The vibration displacement sensor (Vtall-T163R) measures amplitude with an uncertainty of ±1%. The uncertainties of the parameters involved can be calculated using the error transfer formula [12]. The uncertainty of each parameter is summarized in Table 1.

$$\frac{\partial y}{y} = \left[\sum_{i=1}^{n}\left(\frac{\partial \ln f}{\partial x_i}\delta x_i\right)^2\right]^{1/2} \tag{10}$$

Table 1. Uncertainties of parameters

Parameter	Maximum uncertainty
Bulk temperature	±0.1 °C
Wall temperature	±0.2 °C
Pressure	±0.1%
Mass flow	±0.4%
Voltage	±0.1%
Current	±0.2%
Heat flux	±3.2%
Amplitude	±1.0%
Heat transfer coefficient	±5.5%

3. RESULTS AND DISCUSSIONS

To analyze the influence of transverse vibration on the *HTC* of CO_2 at different operating parameters when the test section is placed vertically and horizontally, the mass flux, heat flux, and inlet pressure will be changed for discussion, respectively. Horizontal vibration data is derived from the previous experiments of our research

group [11]. In the figures below, the hollow points represent the static experimental group, and the solid points represent the vibration experimental group.

3.1 Effects of mass flux

Fig. 2 shows the variations of T_w and *htc* at static and vibrating states for mass fluxes of 300, 350, and 400 kg/(m²·s). Other operation conditions are fixed: pressure of 8 MPa, heat flux of 60 kW/m², vibration amplitude and vibration frequency of 800 μm and 30 Hz, respectively. *HTD* occurs in all stationary states; the wall temperature has two peak bulges, and the corresponding *htc* curves have two valleys when the test section is situated vertically. The wall temperature decreases significantly, and correspondingly, the *htc* undergoes a significant enhancement when vibration is applied. This might be attributed to the fact that the vibration disrupts the boundary layer of CO_2 near the wall, causing the near-wall fluid to mix with the mainstream fluid and enabling heat to transfer from the wall to the mainstream region more rapidly. The *HTE* is particularly significant before h_b reaches h_{pc}. When the mass flux is 400 kg/(m²·s), the second temperature peak along the test section vanishes under the vibration reinforcement.

As the mass flux rises, the peak wall temperature drops, and the high-temperature region shortens. This is attributed to the enhanced turbulence intensity and accelerated heat transfer at the wall. This reinforcing effect is especially prominent when h_b ≥300 kJ/kg. In this case, the SCO_2 specific heat is larger, and the fluid's ability to convey heat is enhanced with the rise in the mass flux.

When the test section is horizontally positioned, the wall temperature is lower than when it is placed vertically under identical operating conditions, while *htc* is larger. A peak bulge exists along the channel wall temperature, and there is a peak of *htc* near h_{pc}. Even if the mass flux is 300 kg/(m²·s), the maximum temperature overshoot is 4.9 °C (≤8 °C), and there is no deterioration in heat transfer. Similar to the vertical case, the strengthening effect of vibration is significant in the region of $h_b \le h_{pc}$. When placed horizontally, the vibration strengthening effect is lower than when placed vertically.

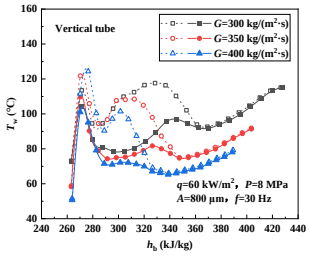

(a)

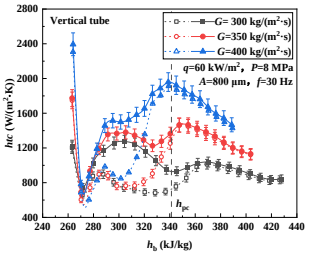

(b)

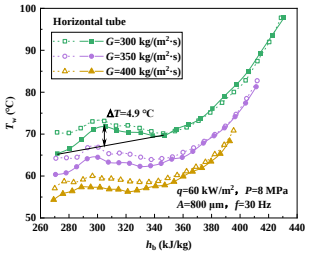

(c)

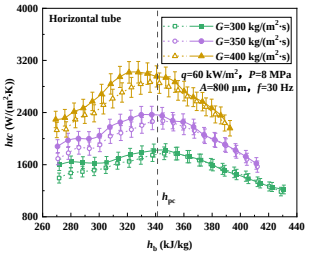

(d)

Fig. 2 Effects of mass flux on heat transfer.

3.2 Effects of heat flux

Fig. 3 shows the variations of T_w and *htc* at static and vibrating states for heat fluxes of 50, 60, and 70 kW/m². Other operating conditions are constant: pressure of 8 MPa, mass flux of 350 kg/(m²·s), vibration amplitude and frequency of 800 μm and 30 Hz, respectively. *HTD* is present in all instances when the test section is placed vertically. T_w significantly decreases and *htc* significantly increases under all heat flux conditions before h_b reaches h_{pc} when vibration is applied; the strengthening effect of vibration is not obvious when h_b is greater than h_{pc}. Under the enhancement of vibration, the second T_w peak along the test section disappears at 70 kW/m².

As the heat flux increases, the T_w ascends, the *htc* decreases, and the high-temperature region widens. When the test section is horizontally positioned, T_w is lower than when it is placed vertically, and the *htc* is greater. At 50 kW/m², the wall temperature bulge disappears. Under all heat fluxes, the *htc* has a peak value near the pseudo-critical enthalpy (h_{pc}). After applying vibration, heat transfer is improved to a certain extent under all conditions.

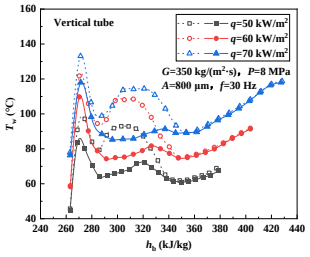

(a)

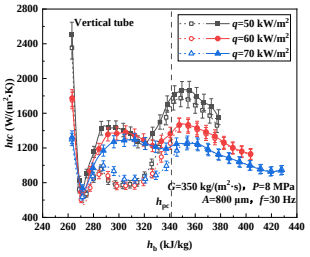

(b)

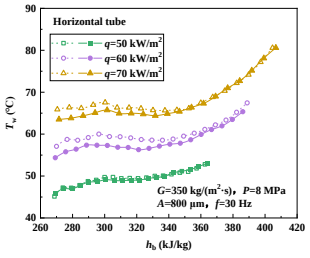

(c)

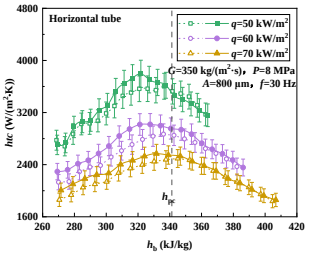

(d)

Fig. 3 Effects of heat flux on heat transfer.

3.3 Effects of pressure

The variation of T_w and *htc* at different pressures is depicted in Fig. 4. The inlet pressures are respectively 7.5 MPa, 8.0 MPa, 9.0 MPa, and 10.0 MPa; Other operating parameters remain constant: a heat flux of 60 kW/m², a mass flux of 350 kg/(m²·s), a vibration amplitude of 800 μm, and a vibration frequency of 30 Hz. The small differences in *htc* at different pressures in the region of h_b < 300 kJ/kg when the test section is placed vertically result from the high fluid temperature near the wall and the slight effect of the pressure on the properties of CO_2. When vibration is applied, T_w decreases significantly and the corresponding *htc* increases significantly. Similarly, the intensification region of vibration is mainly before h_b reaches h_{pc}. The temperature drops significantly in the enhanced region, the influence of pressure on the CO_2 properties increases, and the differences in *htc* under different pressures become larger.

Vibration improves heat transfer in the tube at various pressures when the test section is placed horizontally. The influence of inlet pressure on *htc* is not obvious. The *HTE* effect brought by vibration in the horizontal tube is lower than that in the vertical tube.

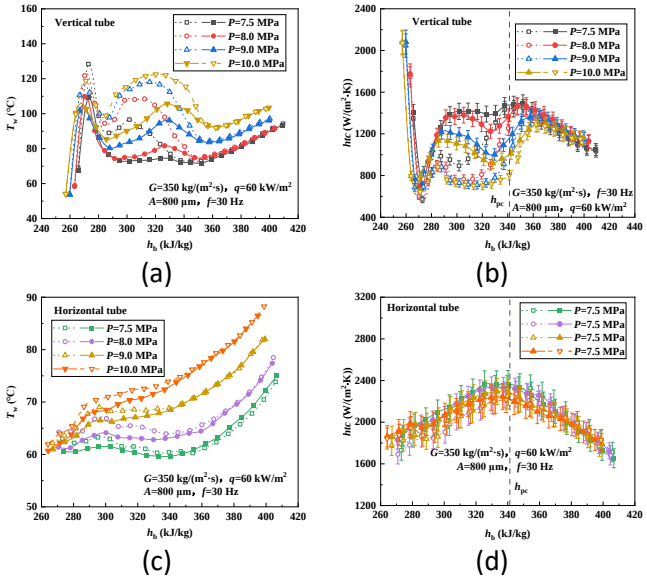

Fig. 4 Effects of pressure on heat transfer.

3.3 Mechanism of vibration-enhanced heat transfer

In this section, the mechanism of vibration-enhanced heat transfer is further analyzed in light of the occurrence of *HTD*: the buoyancy effect and the pseudo-boiling theory.

Based on the experimental data of the vertical tube in Section 3.1, the buoyancy dimensionless number $\overline{Gr}/Re^{2.7}$ is adopted for analysis. The formula is as follows:

$$\overline{Gr} = \frac{(\rho_b - \bar{\rho})\rho_b g d^3}{\mu_b^2} \tag{11}$$

where $\bar{\rho}$ is the average density; it can be calculated by the following equation:

$$\bar{\rho} = \begin{cases} (\rho_w + \rho_b)/2 & T_w < T_{pc} \text{ or } T_b > T_{pc} \\ \dfrac{\rho_b(T_{pc} - T_b) + \rho_w(T_w - T_{pc})}{T_w - T_b} & T_b < T_{pc} < T_w \end{cases} \tag{12}$$

The results are shown in Fig. 5. As the mass flux increases, $\overline{Gr}/Re^{2.7}$ shows a decreasing trend, which proves that increasing the mass flux can weaken the buoyancy force effect and mitigate the *HTD* of SCO_2. In the region before the h_b, the application of vibration has a negligible influence on $\overline{Gr}/Re^{2.7}$. This suggests that vibration is not enhancing heat transfer by weakening the buoyancy force effect.

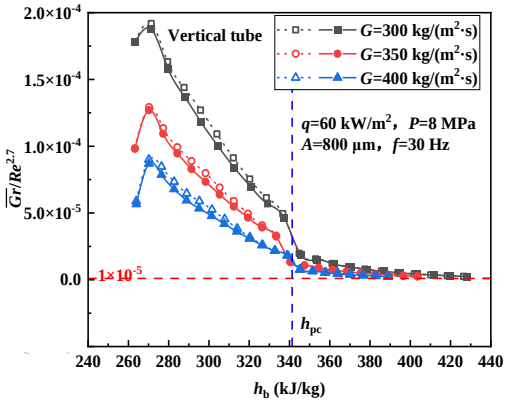

Fig. 5 Variation of $\overline{Gr}/Re^{2.7}$ along the flow channel

The pseudo-boiling theory contends that SCO_2 is not a single phase but can be classified into two states: gas-like and liquid-like. Based on the pseudo-boiling theory, the dimensionless numbers π representing the ratio of the growth rate of the gas-like film to the mainstream velocity and π_{13} representing the temperature gradient inside the near-wall gas-like film are calculated to explain the influence of vibration [13]. The π and π_{13} expressions are as follows:

$$\pi = \frac{q}{G\Delta i}\frac{\rho_l}{\rho_g}, \quad \pi_{13} = \frac{q\beta_{pc}d}{\lambda_g} \tag{13}$$

Where G is the mass flux; ρ_g and ρ_l are the gas-like and liquid-like film densities, both of which have qualitative temperatures of $(T_b+T_{w,i})/2$ and Tb, respectively; Δ_i is the enthalpy of the pseudo-boiling phase change, which needs to be obtained by determining the gas-like and liquid-like *i-T* lines at a given pressure and then intersecting them with the tangent to the enthalpy of SCO_2 at the pseudo-critical temperature. β_{pc} is the expansion coefficient at the pseudo-critical point; λ_g is the thermal conductivity of the gas-like film.

Fig. 6 shows the variation of π and π_{13} at rest and in vibration. There is a peak bulge in π and π_{13} at h_b = 270 kJ/kg. At this time, the growth rate of the gas-like film

accelerates. Meanwhile, a larger π_{13} will cause the gas-like film to blanket the inner wall surface, and the heat accumulates, ultimately leading to *HTD*. This is consistent with Fig. 2. In the region before h_b reaches the h_{pc}, π and π_{13} are significantly reduced under vibration; after h_b reaches the h_{pc}, the results for the stationary and vibration states are close to each other. This indicates that vibration inhibits the growth of the gas-like film near the wall in the region before the h_{pc}, while the smaller temperature gradient of the gas-like film makes it less likely to cover the wall. These two factors enhance the heat transfer between the cold-like liquid of the core and the wall surface, thus mitigating *HTD* and achieving *HTE*.

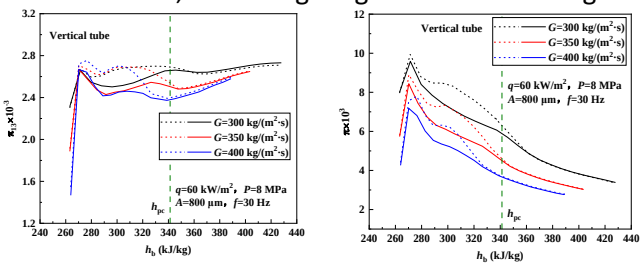

(a) (b)

Fig. 6 Variation of π and π_{13} along the flow channel

4. CONCLUSIONS

In this paper, the effects of transverse vibration on the *HTC* of SCO_2 in vertical and horizontal tubes are investigated experimentally. The main conclusions are summarized as follows:

(1) The experimental results demonstrate that vibration can enhance heat transfer. In the vertical tube, vibration can mitigate *HTD*, weaken the second peak of the T_w along the channel significantly, and amplify *htc*, while improving heat transfer in horizontal tubes. It is found that vibration enhancement mainly acts in the region before h_b reaches the h_{pc}.

(2) Heat transfer performance is preferred at higher mass flux or lower heat flux in both horizontal and vertical tubes. A smaller inlet pressure enhances the *HTC* of SCO_2 in the vertical tube but has little effect on the *htc* of the horizontal tube.

(3) Based on the buoyancy effect and the pseudo-boiling theory, the dimensionless numbers $\overline{Gr}/Re^{2.7}$, π and π_{13} are calculated to analyze vibration intensification. It is found that vibration achieves *HTE* not by weakening the buoyancy force effect but by suppressing the growth of the gas-like film near the wall as well as the internal temperature gradient, which in turn enhances the heat transfer between the mainstream liquid fluid and the wall.

ACKNOWLEDGEMENT

The authors gratefully acknowledge the Major Science and Technology Project in Anhui Province (Grant No. 202203a07020023).

REFERENCE

[1] J. Xu, C. Liu, E. Sun, J. Xie, M. Li, Y. Yang, J. Liu, Perspective of S−CO2 power cycles, Energy, 186(2019) 115831.

[2] L. Han, J. Chen, R. Zhao, H. Chen, W. Cheng, Thermal conductivity measurements for CO2 near the pseudo-critical line based on cluster data processing method, Int. Commun. Heat Mass, 156(2024) 107600.

[3] X.-L. Li, X.-Y. Yu, P.-T. Liu, Y.-H. Fan, D.-L. Yang, G.-H. Tang, S-CO2 flow in vertical tubes of large-diameter: Experimental evaluation and numerical exploration for heat transfer deterioration and prevention, Int. J. Heat Mass Tran., 216(2023) 124563.

[4] X. Lei, J. Zhang, L. Gou, Q. Zhang, H. Li, Experimental study on convection heat transfer of supercritical CO2 in small upward channels, Energy, 176(2019) 119-130.

[5] P. Jiang, Y. Zhang, C. Zhao, R. Shi, Convection heat transfer of CO2 at supercritical pressures in a vertical mini tube at relatively low reynolds numbers, Exp. Therm. Fluid Sci., 32(2008) 1628-1637.

[6] Y. Bae, H. Kim, D. Kang, Forced and mixed convection heat transfer to supercritical CO2 vertically flowing in a uniformly-heated circular tube, Exp. Therm. Fluid Sci., 34(2010) 1295-1308.

[7] X. Xu, C. Liu, C. Dang, Y. Wu, X. Liu, Experimental investigation on heat transfer characteristics of supercritical CO2 cooled in horizontal helically coiled tube, International Journal of Refrigeration, 67(2016) 190-201.

[8] S. Zhang, X. Xu, C. Liu, X. Liu, Z. Ru, C. Dang, Experimental and numerical comparison of the heat transfer behaviors and buoyancy effects of supercritical CO2 in various heating tubes, Int. J. Heat Mass Tran., 149(2020) 119074.

[9] J. Chen, R. Zhao, Y. Nian, W. Cheng, Numerical study on the effects of cylindrical roughness on heat transfer performance and entropy generation of supercritical carbon dioxide in vertical tubes, Int. J. Heat Mass Tran., 208(2023) 124060.

[10] J. Chen, L. Han, H. Chen, W. Cheng, Study on heat transfer characteristics and enhancement mechanism of supercritical carbon dioxide in adaptive channels, Appl. Therm. Eng., 253(2024) 123761.

[11] K. Wang, J. Chen, R. Zhao, W. Cheng, Experimental investigation of the effects of transverse vibration on the supercritical CO2 heat transfer characteristics in horizontal tubes, Int. J. Heat Mass Tran., 214(2023) 124311.

[12] R.-J. Moffat, Describing the uncertainties in experimental results, Exp. Therm. Fluid Sci., 1(1988) 3-17.

[13] H. Zhang, J. Xu, X. Zhu, Dimensional analysis of flow and heat transfer of supercritical CO_2 based on pseudo-boiling theory, Acta Phys. Sin.-Ch Ed, 70(2021) 44401.